

Role of the inner copper-oxide plane in interlayer Josephson effects in multi-layered cuprate superconductors

Y. Nomura¹, R. Okamoto¹, T. Mizuno¹, S. Adachi²,
T. Watanabe², M. Suzuki¹, and I. Kakeya¹

¹*Department of Electronic Science and Engineering. Kyoto University, Kyoto, Japan*

²*Graduate school of Science and Technology,
Hirosaki University, Hirosaki, Japan*

(Dated: March 4, 2022)

Abstract

We find systematic signatures suggesting a different superconducting nature for a triple-layered cuprate $\text{Bi}_2\text{Sr}_2\text{Ca}_2\text{Cu}_3\text{O}_{10+\delta}$ with respect to a double-layer through the properties of intrinsic Josephson junctions (IJJs). Our measurements on the current-voltage characteristics reveal that the c -axis maximum Josephson current density is sensitive to the superfluid density in outer planes while the critical temperature and the superconducting gap remain unaffected. Switching dynamics of stacked IJJs exhibit that the fluctuation in gauge-invariant phase difference of an IJJ implies that the inner plane completely shields the capacitive coupling between adjacent IJJs, which is essential for mono- and bilayered cuprates.

Cuprate superconductors have been widely debated for the past three decades. Particularly, the underlying mechanism that determines the critical temperature (T_c) and methods to increase T_c have received much attention. An essential ingredient that determines T_c is the number of CuO_2 planes (n) composing superconducting layers (SLs) that are separated by blocking layers (BLs). It is known that T_c increases with increasing n for identical BLs in the crystal structure. T_c reaches its maximum value for $n = 3$, beyond which it decreases with increasing n^1 . This is attributed to an insufficient carrier doping in inner planes (IPs) from BLs due to the presence of outer planes (OPs)^{2,3}, resulting in inequivalent superconducting gaps Δ of OP and IP^{4,5}.

This inequivalent Δ arises issues on the relevance between T_c and the maximum c -axis supercurrent J_c in these trilayer materials because the low-energy electrostatics along the c -axis of cuprate superconductors are mostly described by the Josephson tunnelings between SLs⁶⁻¹¹. Moreover, in conventional superconductors, the maximum Josephson current is known to be determined by the superconducting gap of superconducting electrodes¹². However, in bilayer $\text{Bi}_2\text{Sr}_2\text{CaCu}_2\text{O}_{8+\delta}$ (Bi2212), the representative material of intrinsic Josephson junctions (IJJs), the doping evolution of J_c shows anti-correlation with that of Δ ¹³. Although doping evolutions of Δ and J_c in trilayer $\text{Bi}_2\text{Sr}_2\text{Ca}_2\text{Cu}_3\text{O}_{10+\delta}$ have been reported, the effect of the inequivalent Δ is smeared because of unwanted Bi2212 layers included in the samples¹⁴. The distribution of Δ in SLs are essential for intralayer electrostatics, which have been observed in the infrared frequency regions in $\text{YBa}_2\text{Cu}_3\text{O}_7$ (YBCO)^{15,16}. In multi-layered cuprates, multiple intralayer plasmons corresponding to different combinations between adjacent CuO_2 planes have also been observed¹⁷. Quite recently, Okamoto et al argue that the capacitive coupling^{9,18} plays an essential role for the intralayer Josephson coupling¹⁹ in the context of the light-enhanced superconductivity²⁰.

In this letter, we discuss the peculiarities of a trilayer cuprate superconductor in comparison to mono- and bilayer cuprates through measurements of the Josephson critical current density (J_c), the superconducting gap (Δ), and the Josephson switching rate ($\Gamma(I)$). The measurements were performed on several mesa-structured samples of Bi2223 with a few IJJs of planar area $S = 1.0\mu\text{m}^2$ as illustrated in Fig. 1(a) and experimental details are described in Supplementary Materials²¹. We have found specific features for Bi2223 on the proximity effect of the triple-layered superconducting layer and the doping evolution of J_c . The systematic difference between the phase-fluctuation temperature (T_{eff}) extracted from $\Gamma(I)$

of the two topmost IJJs in Bi2223 compared to Bi2212 illuminates the role of capacitive coupling between adjacent IJJs^{9,18}. These findings stimulate the development of a new intrinsic Josephson junction model that includes electrostatics between CuO₂ planes inside a superconducting layer of Bi-cuprates, which has been considered to be quenched.

First, we discuss a proximity effect for the triple CuO₂ planes found in the maximum Josephson current of the surface IJJ. A current-voltage characteristic (IVC) of sample M at 0.4 K is shown in Fig. 2 (a). The values of J_c for first and second switches (labeled as FS and SS) of sample M are $J_{c1} = 1.4$ and $J_{c2} = 1.45$ kA/cm², respectively. In Bi2212 mesa structures, J_c of the first IJJ (IJJ1) is commonly reduced more than tens percent of the J_c of other bulk IJJs (IJJ2)^{21,22}. This is due to the proximity effect to the normal electrode evaporated just above IJJ1^{23,24}. However, in Bi2223, this reduction is significantly smeared. We attribute this change of the reduction in J_c to the presence of IPs. In cuprate superconductors with the d -wave symmetry of superconducting gap, superfluid density ρ_s determines both T_c ^{25,26} and J_c because carrier doping significantly influences to the extent of the Fermi arc in the k -space and consequently alters superconducting properties even for cases with an identical superconducting gap²⁷⁻³⁰. Here, SLs (double and triple CuO₂ planes for Bi2212 and Bi2223, respectively) are numbered from the top to the bottom as SL1, SL2, etc., and CuO₂ planes are labeled as UOP1, IP1, and LOP1 for the case of SL1 in Bi2223, as shown in Fig. 1 (a,b). BLs are also numbered as BL1, BL2, etc. similar to SLs. In Bi2212, as depicted in Fig. 1 (c), Cooper pairs in UOP1 (closest to the normal metal electrode) mainly contribute to the diffusion and Cooper pairs in LOP1 are less but considerably diffused. As a result, the penetration of ρ_s into underlying BLs is significantly reduced. In Bi2223, IP1 plays the role of the LOP1 in Bi2212. Thus ρ_s in the third CuO₂ plane (which is LOP1) is much less influenced. Therefore, the J_c of a multilayered IJJ is determined by a combination of ρ_s in a pair of OPs sandwiching a BL (viz. LOP1–UOP2 and LOP2–UOP3 for J_{c1} and J_{c2} , respectively).

Second, we exhibit that chemical disorder of the Sr site significantly reduces ρ_s of OPs irrespective to T_c . Figure 2 (d) shows J_{c2} as a function of doping (p) estimated from bulk critical temperature T_{c2} through an empirical formula³¹ with an assumption of the optimum T_{c2} of 107 K¹⁴. Although the relationship is relied on mono- and bilayer cuprates, the formula is valid to express relative difference in doping of underdoped trilayer cuprates³². It is clearly seen that the mean J_{c2} of samples K and L is considerably lower than samples

of M and N despite their higher T_c . One can infer two exponential doping evolutions in J_c corresponding to the difference in Bi/Sr chemical compositions of crystals. This is in sharp contrast to the case of Bi2212, where the doping evolution of J_c falls into a single exponential dependence irrespective of the difference in Bi/Sr ratios¹³. It is known that Bi2212 and Bi2201 crystals with Sr concentration below 2.0 tend to have a lower optimum T_c than perfectly stoichiometric crystals. The disorder in CuO_2 planes, induced by the partial substitution of Bi at the Sr sites adjacent to the CuO_2 plane, reduces T_c ³³. In the present study on Bi2223, OPs of batch A (samples J, K, and L) are more disordered than OPs of batch B (samples M, M', and N) because more Sr are substituted for Bi in batch A²¹. We consider this as a reason for lower J_c of mesas K and L compared to mesas M and N with an anti-correlation between J_c and T_c . The present results, nevertheless, show that T_c of Bi2223 is not likely governed by the disorder of the CuO_2 planes. Although no complete doping evolutions of J_c and T_c have been clarified in this work, a simple comparison between batches A and B implies that J_c is determined by both the doping and disorder of OP whereas T_c is determined by doping of IP.

The disorder of the Sr site does not affect to the magnitude of the superconducting gap. We have performed intrinsic tunneling spectroscopy in samples J and M'. Quasiparticle dI/dV vs V spectra of sample M' are shown in Fig. 2 (b). The obtained $2\Delta = 83$ meV at $T = 5$ K of the sample M' is roughly consistent with the published $2\Delta = 82$ meV by Yamada et al.¹⁴ for $T_c = 96$ K in the $10 \times 10 \mu\text{m}^2$ and $N \sim 10$ mesa made of a crystal with identical nominal composition to batch A and slight Bi2212 intergrowth impurities. The obtained Δ is close to the smaller superconducting gap of 35 meV obtained by point contact measurements for a crystal with $T_c = 101$ K⁵. Comparing with ARPES data from OP, our Δ is considerably smaller than the nodal gap ~ 50 meV⁴. Furthermore, the proximity effect from the Ag electrode is not presumed to reduce the amplitude of superconducting gap of UOP1. Quasiparticle tunneling spectra between superconductors with different superconducting gaps Δ_1 and Δ_2 exhibit two dI/dV peaks at $eV = \Delta_1 + \Delta_2$ and $|\Delta_1 - \Delta_2|$ ³⁴. In the present study, however, such a signature is not found even for the second-order derivative d^2I/dV^2 , as shown in Fig. 2 (c). Thus we conclude that the proximity effect reduces carrier concentrations of CuO_2 planes of SL1 and results in the decrease in J_{c1} . Spectroscopic measurements such as ARPES and STM to determine superconducting gap and carrier density in the momentum space will validate our arguments.

The difference of intralayer electrodynamics between bi- and trilayer cuprates is illuminated by fluctuation measurements of the Josephson switching of an individual IJJ more explicitly in terms of the capacitive coupling between adjacent IJJs because its length scale is the order of 1 nm in BSCCOs⁹. The Josephson switching rate $\Gamma(I)$ consists of quantum ($\Gamma_Q \propto \exp[-\omega_p^{-1}]$) and thermal ($\Gamma_T \propto \exp[-T^{-1}]$) contributions, where ω_p and T are the Josephson plasma frequency and temperature of the system, respectively^{21,35,36}. Figure 2 (e) shows phase-fluctuation temperature T_{eff} and fluctuation-free critical current density J_{c0} of FS and SS in sample M as functions of bath temperature T_{bath} together with the data in Bi2212²². $T_{\text{eff}} - T_{\text{bath}}$ behaviors for FS and SS are very similar in Bi2223 while T_{eff} for SS is much higher than T_{eff} for FS in the saturated low-temperature region $T_{\text{bath}} < 1$ K in Bi2212 despite of their similar J_{c0} of SS as shown in the inset of Fig. 2 (e). These are common among 4 Bi2223 mesas and 4 Bi2212 mesas with identical lateral size^{21,37}. Thus we suggest a naive conclusion that quantum fluctuation, ω_p , of SS is not enhanced in trilayer cuprates in contrast to mono- and bilayer cuprates^{22,38}.

This absence of the enhancement in ω_p is presumed to be attributed to a reduction of the capacitive coupling in Bi2223 through the following considerations. It is noted that the possibility of heating as the origin of the increased ω_p for SS of Bi2201 and Bi2212 is certainly excluded by a counterintuitive behavior in sample M that the saturated T_{eff} for SS ($T_2^* = 2.0$ K) is slightly lower than that for FS ($T_1^* = 2.3$ K). T_2^*/T_1^* roughly corresponds to the enhancement factor of ω_p . In the presence of the capacitive coupling, IJJ2 couples with the Josephson oscillation $\omega_J = 2eV/\hbar$ of IJJ1 on the verge of SS, where V is the applied voltage to IJJ1. Here, IVCs offer $\omega_J/2\pi \simeq 12$ and 20 THz for Bi2212 and Bi2223, respectively. Assuming an SL being a uniform superconducting electrode, IJJ1 directly couples to IJJ2. Josephson coupling energy $E_J = \hbar J_{c0} S/2e$ of IJJ2 (~ 10 THz) is smaller than $\hbar\omega_J$ for both Bi2212 and Bi2223, thus the Josephson radiation results in excitations to continuous energy state out of the *hollow* of tilted washboard potential. This is an analogue of the photovoltaic effect. The Josephson radiation to IJJ2 of Bi2223 damps to the factor of 0.3 – 0.5 in comparison with the case of Bi2212 because of increase in screening superfluid carriers in SL2.

An introduction of the intralayer Josephson coupling explains the phenomena more microscopically. The lowest intralayer Josephson plasmons lie at 14 and 15 THz for Bi2212³⁹ and Bi2223⁴⁰, respectively. The Josephson oscillation of IJJ1 may couple to the intralayer

plasmons under a current bias. In the bilayer case, the intralayer plasmon of SL2 directly couples to the Interlayer plasmon of IJJ2. However in the trilayer case, the intralayer plasmon between UOP2 and IP2 is necessary to excite another intralayer plasmon between IP2 and LOP2 to couple to IJJ2. This complicated process to couple between IJJ1 and IJJ2 is presumed to make the enhancement of the quantum fluctuation of IJJ2 invalid. Thus we claim that the presence of IP provides significant difference of capacitive coupling in Bi2223 from those in Bi2201 and Bi2212.

Recent observations of the light-induced superconductivity in YBCO up to room temperatures²⁰ have been investigated theoretically by Okamoto et al.¹⁹. In their model, the capacitive coupling between the CuO₂ planes within a SL is taken into consideration on the basis of the alternating IJJ model⁴¹. They propose that the moderate capacitive coupling between the bilayer of YBCO contribute to enhanced interlayer Josephson coupling. However, in Bi2223, light-induced superconductivity at temperatures higher than its equilibrium T_c has not been observed⁴². This scenario is totally consistent to our results described above.

In summary, the localized picture of superfluid density ρ_s in CuO₂ planes explains the qualitative differences of the Josephson maximum currents and the superconducting gaps between Bi2212 and Bi2223. The behavior of the phase-fluctuation revealed that the inner CuO₂ plane of Bi2223 shields the capacitive coupling between IJJs. These specific features in Bi2223 propose a new model to describe the c -axis conductivity of multi-layered cuprates more precisely.

ACKNOWLEDGMENTS

This work was partly supported by Grant-in-Aid for JSPS Fellows No. 16J11491. We thank Osamu Sakai at University of Shiga Prefecture for allowing us to use the electron-beam lithography facility.

¹ A. Iyo, Y. Tanaka, H. Kito, Y. Kodama, P. M. Shirage, D. D. Shivagan, H. Matsuhata, K. Tokiwa, and T. Watanabe, Journal of the Physical Society of Japan **76**, 094711 (2007).

² A. Trokiner, L. L. Noc, J. Schneck, A. M. Pougnet, R. Mellet, J. Primot, H. Savary, Y. M. Gao, and S. Aubry, Phys. Rev. B **44**, 2426 (1991).

- ³ H. Kotegawa, Y. Tokunaga, K. Ishida, G.-q. Zheng, Y. Kitaoka, H. Kito, A. Iyo, K. Tokiwa, T. Watanabe, and H. Ihara, *Physical Review B* **64**, 064515 (2001).
- ⁴ S. Ideta, K. Takashima, M. Hashimoto, T. Yoshida, A. Fujimori, H. Anzai, T. Fujita, Y. Nakashima, A. Ino, M. Arita, H. Namatame, M. Taniguchi, K. Ono, M. Kubota, D. H. Lu, Z. X. Shen, K. M. Kojima, and S. Uchida, *Phys. Rev. Lett.* **104**, 227001 (2010).
- ⁵ R. Sekine, K. Ogata, A. Tsukada, and N. Miyakawa, *Physics Procedia* **58**, 82 (2014).
- ⁶ R. Kleiner, F. Steinmeyer, G. Kunkel, and P. Müller, *Phys. Rev. Lett.* **68**, 2394 (1992).
- ⁷ K. Tamasaku, Y. Nakamura, and S. Uchida, *Physical Review Letters* **69**, 1455 (1992).
- ⁸ Y. Matsuda, M. Gaifullin, K. Kumagai, K. Kadowaki, and T. Mochiku, *Physical Review Letters* **75**, 4512 (1995).
- ⁹ T. Koyama and M. Tachiki, *Phys. Rev. B* **54**, 16183 (1996).
- ¹⁰ M. Suzuki, T. Watanabe, and A. Matsuda, *Physical Review Letters* **81**, 4248 (1998).
- ¹¹ I. Kakeya, K. Kindo, K. Kadowaki, S. Takahashi, and T. Mochiku, *PHYSICAL REVIEW B* **57**, 3108 (1998).
- ¹² V. Ambegaokar and A. Baratoff, *Physical Review Letters* **11**, 104 (1963).
- ¹³ M. Suzuki, T. Hamatani, K. Anagawa, and T. Watanabe, *Physical Review B* **85**, 214529 (2012).
- ¹⁴ Y. Yamada, K. Anagawa, T. Shibauchi, T. Fujii, T. Watanabe, A. Matsuda, and M. Suzuki, *Phys. Rev. B* **68**, 054533 (2003).
- ¹⁵ S. Tajima, G. D. Gu, S. Miyamoto, A. Odagawa, and N. Koshizuka, *Physical Review B* **48**, 16164 (1993).
- ¹⁶ K. M. Kojima, S. Uchida, Y. Fudamoto, and S. Tajima, *Physical Review Letters* **89**, 247001 (2002).
- ¹⁷ Y. Hirata, K. Kojima, M. Ishikado, S. Uchida, A. Iyo, H. Eisaki, and S. Tajima, *Physical Review B* **85**, 054501 (2012).
- ¹⁸ M. Machida, T. Koyama, and M. Tachiki, *Phys. Rev. Lett.* **83**, 4618 (1999).
- ¹⁹ J.-i. Okamoto, A. Cavalleri, and L. Mathey, *Physical Review Letters* **117**, 227001 (2016).
- ²⁰ W. Hu, S. Kaiser, D. Nicoletti, C. R. Hunt, I. Gierz, M. C. Hoffmann, M. Le Tacon, T. Loew, B. Keimer, and A. Cavalleri, *Nat. Mater.* **13**, 705 (2014), arXiv:1308.3204.
- ²¹ “Supplemental materials for the present manuscript.”.
- ²² Y. Nomura, R. Okamoto, and I. Kakeya, *Superconductor Science and Technology* **30**, 105001 (2017).

- ²³ A. K. Gupta, L. Cretinon, N. Moussy, B. Pannetier, and H. Courtois, Phys. Rev. B (Condensed Matter) **69**, 104514 (2004).
- ²⁴ M. Suzuki, M. Ohmaki, R. Takemura, K. Hamada, T. Watanabe, K. Ota, H. Kitano, and A. Maeda, J. of Phys.: Conf. Ser. **129**, 012033 (2008).
- ²⁵ Y. J. Uemura, L. P. Le, G. M. Luke, B. J. Sternlieb, W. D. Wu, J. H. Brewer, T. M. Rise-
man, C. L. Seaman, M. B. Maple, M. Ishikawa, D. G. Hinks, J. D. Jorgensen, G. Saito, and
H. Yamochi, Phys. Rev. Lett. **66**, 2665 (1991).
- ²⁶ C. C. Homes, S. V. Dordevic, M. Strongin, D. A. Bonn, and R. Liang, Nature **430**, 539 (2004).
- ²⁷ A. Kanigel, M. R. Norman, M. Randeria, U. Chatterjee, S. Souma, A. Kaminski, H. M. Fretwell,
S. Rosenkranz, M. Shi, T. Sato, T. Takahashi, Z. Z. Li, H. Raffy, K. Kadowaki, D. Hinks,
L. Ozyuzer, and J. C. Campuzano, Nature Physics **2**, 447 (2006).
- ²⁸ W. S. Lee, I. M. Vishik, K. Tanaka, D. H. Lu, T. Sasagawa, N. Nagaosa, T. P. Devereaux,
Z. Hussain, and Z.-X. Shen, Nature **450**, 81 (2007).
- ²⁹ T. Yoshida, X. J. Zhou, K. Tanaka, W. L. Yang, Z. Hussain, Z. Shen, A. Fujimori, S. Sahrakorpi,
M. Lindroos, R. S. Markiewicz, A. Bansil, S. Komiya, Y. Ando, H. Eisaki, T. Kakeshita, and
S. Uchida, Physical Review B **74**, 224510 (2006).
- ³⁰ H. Kambara, I. Kakeya, and M. Suzuki, Phys. Rev. B **87**, 214521 (2013).
- ³¹ J. L. Tallon, C. Bernhard, H. Shaked, R. L. Hitterman, and J. D. Jorgensen, Phys. Rev. B **51**,
12911 (1995).
- ³² D. T. Jover, R. J. Wijngaarden, R. Griessen, E. M. Haines, J. L. Tallon, and R. S. Liu, Phys.
Rev. B **54**, 10175 (1996).
- ³³ H. Eisaki, N. Kaneko, D. L. Feng, A. Damascelli, P. K. Mang, K. M. Shen, Z.-X. Shen, and
M. Greven, Physical Review B **69**, 064512 (2004).
- ³⁴ E. L. Wolf, *Principles of Electron Tunneling Spectroscopy: Second Edition* (Oxford : Oxford
University Press, 2012).
- ³⁵ H. Kramers, Physica **7**, 284 (1940).
- ³⁶ A. O. Caldeira and A. J. Leggett, Phys. Rev. Lett. **46**, 211 (1981).
- ³⁷ Y. Nomura, T. Mizuno, H. Kambara, Y. Nakagawa, T. Watanabe, I. Kakeya, and M. Suzuki,
J. Phys.: Conf. Ser. **507**, 012038 (2014).
- ³⁸ Y. Nomura, T. Mizuno, H. Kambara, Y. Nakagawa, and I. Kakeya, J. Phys. Soc. Jpn. **84**,
013704 (2015).

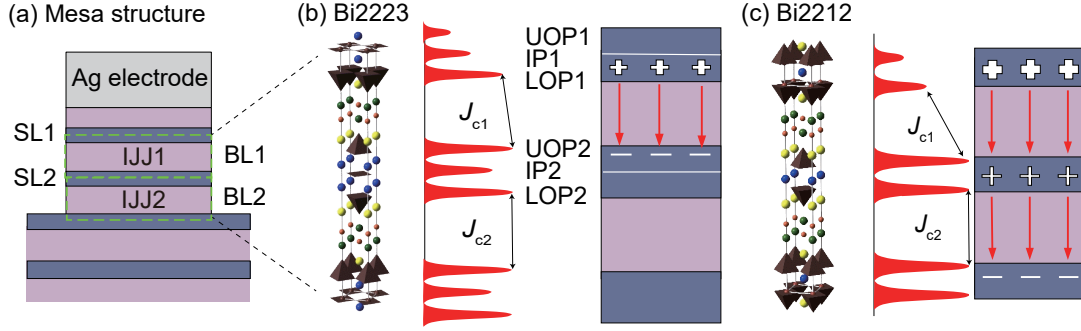


FIG. 1. (a) Cross-sectional schematic view of the mesa. (b) For Bi2223, crystal structure corresponding to the mesa cross section, sketch of distribution of superfluid density ρ_s and schematic illustration of capacitive coupling from left to right. (c) Corresponding illustrations for Bi2212.

³⁹ V. Železný, S. Tajima, D. Munzar, T. Motohashi, J. Shimoyama, and K. Kishio, Phys. Rev. B **63**, 060502 (2001).

⁴⁰ A. V. Boris, D. Munzar, N. N. Kovaleva, B. Liang, C. T. Lin, A. Dubroka, A. V. Pimenov, T. Holden, B. Keimer, Y.-L. Mathis, and C. Bernhard, Phys. Rev. Lett. **89**, 277001 (2002).

⁴¹ T. Koyama, J. Phys. Soc. Jpn. **71**, 2986 (2002).

⁴² W. Hu, D. Nicoletti, A. V. Boris, B. Keimer, and A. Cavalleri, Phys. Rev. B **95**, 104508 (2017).

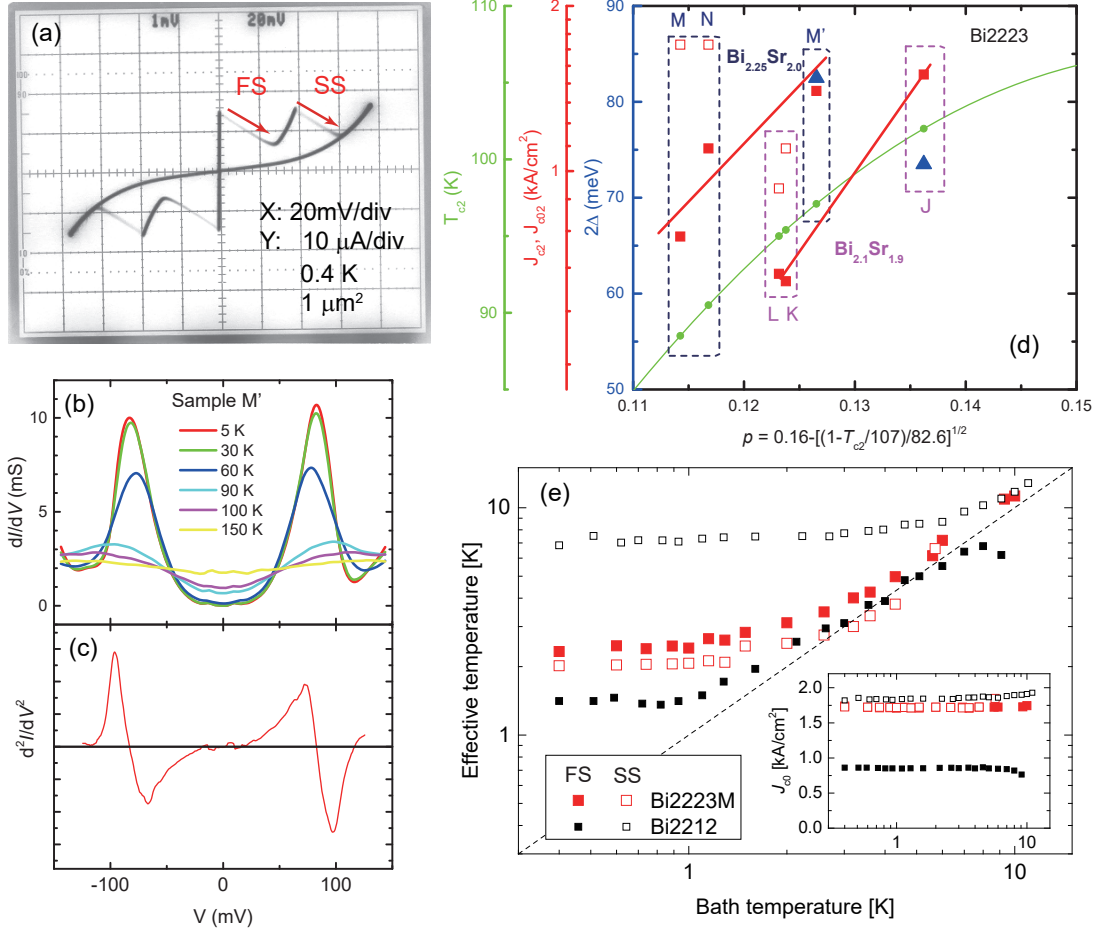


FIG. 2. (a) IVCs of sample M at 0.4 K. IJJ1 and IJJ2 switch at FS and SS, respectively. (b,c) dI/dV spectra and the derivative (at 5 K) of mesa M'. dI/dV spectra quantitatively corresponds to quasiparticle density of states thus the remarkable peaks below T_c and minimum at $V = 0$ are due to opening the superconducting gap and pseudogap. No signature implying the presence of different superconducting gap is seen. Small wiggling close to $V = 0$ is due to incomplete suppression of Josephson current. (d) Doping evolution of mean value in critical current density of SS J_{c2} (red squares), fluctuation-free critical current density of SS J_{c02} (red open squares), T_c (green circles), and superconducting gap 2Δ (blue triangles) for the second IJJs of Bi2223. Two lines for different cation concentrations are drawn for J_{c2} vs p . (e) The relation between T_{eff} and T_{bath} for FS (solid) and SS (open) for sample M (red) and Bi2212 mesa C of Ref.²² (black). In Bi2223, T_{eff} of the both switches is independent of temperature below 1 K and $T_{\text{eff}} \approx T_{\text{bath}}$ holds above 2.0 K. In Bi2212, T_{eff} for SS is much higher than that of FS at low temperature region. In the inset, temperature dependence of fluctuation-free critical current densities J_{c0} are plotted with the same symbols.